Effect of nonadiabatic electronic-vibrational interactions on the transport properties of single-molecule junctions

A. Erpenbeck,[1] R. Härtle,[2] and M. Thoss[1]

[1]*Institut für Theoretische Physik und Interdisziplinäres Zentrum für Molekulare Materialien, Friedrich-Alexander-Universität Erlangen-Nürnberg, Staudtstrasse 7/B2, D-91058 Erlangen, Germany*

[2]*Institut für Theoretische Physik, Georg-August-Universität Göttingen, Friedrich-Hund-Platz 1, D-37077 Göttingen, Germany*

The interaction between electronic and vibrational degrees of freedom in single-molecule junctions may result from the dependence of the electronic energies or the electronic states of the molecular bridge on the nuclear displacement. The latter mechanism leads to a direct coupling between different electronic states and is referred to as nonadiabatic electronic-vibrational coupling. Employing a perturbative nonequilibrium Green's function approach, we study the influence of nonadiabatic electronic-vibrational coupling in model molecular junctions. Thereby, we distinguish between systems with well-separated and quasidegenerate electronic levels. The results show that the nonadiabatic electronic-vibrational interaction can have a significant influence on the transport properties. The underlying mechanisms, in particular the difference between nonadiabatic and adiabatic electronic-vibrational couplings, are analyzed in some detail.

I. INTRODUCTION

Quantum transport in nanostructures is an active field of experimental and theoretical research. Among the variety of architectures investigated, single-molecule junctions, that is, a single molecule chemically bound to two macroscopic leads, have been of great interest recently [1–9]. These systems combine the possibility to study fundamental aspects of nonequilibrium many-body quantum physics at the nanoscale with the perspective for applications in nanoelectronic devices [10–14]. Studies of transport in molecular junctions have revealed a variety of interesting transport phenomena, such as rectification [15–19], switching [6,20–25], quantum interference [26–33], and negative differential resistances [19,34–43].

An important mechanism in electron transport across a molecular bridge is the coupling between the electronic and nuclear degrees of freedom [44]. Due to the small size of molecules, transport-induced charge fluctuations influence the nuclear geometry. This leads to vibrational structures in the conductance of a molecular junction, current-induced vibrational excitation, and a variety of interesting nonequilibrium effects [9,19,39,45–50]. A well-studied mechanism in this context is polaron-type transport, which results from the state-specific dependence of the electronic energies of the molecule on the nuclear displacement, which cause, e.g., a change of the potential-energy surface of the molecular bridge upon charging of the molecule [19,44]. In addition, due to the dependence of the electronic states on the nuclear coordinates, the kinetic-energy operator of the nuclei may cause transitions between different electronic states, which can influence the transport properties profoundly. This mechanism, which represents a breakdown of the Born-Oppenheimer approximation, is referred to as nonadiabatic electronic-vibrational coupling [51,52] and has recently been investigated, e.g., in the context of the Jahn-Teller effect in molecular junctions [53–56] and in scanning tunneling microscopy (STM) studies of oligothiophene molecules on a Au substrate [57]. It also manifests itself in the off-resonant transport regime in structures in inelastic electron tunneling spectra (IETS) [58–61]. In the

present paper, we provide a model-based analysis of the mechanism of nonadiabatic electronic-vibrational coupling in molecular junctions transport and its interplay with polaron-type transport. Thereby, we focus on the resonant transport regime, where the effects of electron-vibrational coupling are typically more pronounced.

A variety of different approaches have been used to describe vibrationally coupled electron transport in molecular junctions and other nanostructures, including density-matrix approaches [19,46,50,62–64], scattering theory [65–68], path integrals [69,70], multiconfigurational wave-function methods [50,71], mixed quantum-classical and semiclassical approaches [72,73], and nonequilibrium Green's functions theory [44,48,50,74–82]. In this work, we will apply the latter approach in combination with the self-consistent Born approximation to characterize transport in molecular junctions.

The outline of this paper is as follows: In Sec. II we introduce the model and the nonequilibrium Green's function approach used to describe vibrationally coupled transport through a molecular junction. Section III presents results for selected model systems and an analysis of the basic effects of nonadiabatic electronic-vibrational coupling. Thereby, we distinguish between molecules with well-separated (Sec. III A) and quasidegenerate (Sec. III B) electronic states. Section IV concludes with a summary.

II. THEORETICAL METHODOLOGY

A. Model Hamiltonian

We consider charge transport through a molecule attached to two macroscopic leads. The molecule is described by the model Hamiltonian H_{Mol}, consisting of a set of electronic states and vibrational modes

$$H_{\text{Mol}} = \sum_{\alpha} \hbar\Omega_{\alpha} a_{\alpha}^{\dagger} a_{\alpha} + \sum_{i} \epsilon_{i} d_{i}^{\dagger} d_{i} + \sum_{\alpha i j} M_{ij}^{\alpha} Q_{\alpha} d_{i}^{\dagger} d_{j}. \quad (1)$$

Here, $\hbar\Omega_{\alpha}$ is the energy of vibrational mode α described within the harmonic approximation and with the corresponding

creation and annihilation operators, $a_\alpha^\dagger$ and a_α, and nuclear displacement $Q_\alpha = (a_\alpha + a_\alpha^\dagger)/\sqrt{2}$. Analogously, ϵ_i is the energy of the molecular electronic state i with creation and annihilation operators $d_i^\dagger$ and d_i. In our model, we neglect the spin of the electrons, electron-electron interactions, and electronic-vibrational interaction of higher order in the nuclear displacement.

The interaction between the electronic and vibrational degrees of freedom of the molecular bridge is described by the last term of Eq. (1) with coupling strengths M_{ij}^α. The electronic-vibrational interaction can be separated into two different types of contributions: (i) diagonal terms $M_{ii}^\alpha Q_\alpha d_i^\dagger d_i$, which depend only on the population of the electronic states, and (ii) nondiagonal terms $M_{ij}^\alpha Q_\alpha d_i^\dagger d_j$, $i \neq j$, which describe transitions between different electronic states of the molecule induced by coupling to the vibrational degrees of freedom.

The separation of the different terms depends on the chosen electronic basis. In first-principles treatments, often, the electronic eigenstates of the molecular bridge are employed; i.e., a so-called adiabatic basis set is used. In such a basis, the dependence of the electronic energies on the nuclear coordinates results (within the linear approximation) in a diagonal term similar to $M_{ii}^\alpha Q_\alpha d_i^\dagger d_i$, and furthermore, nondiagonal terms would not be present. This treatment corresponds to the adiabatic or Born-Oppenheimer approximation [52,83]. Without coupling to the leads, the resulting molecular Hamiltonian can be diagonalized using the polaron transformation [19,46,80,84,85]. Within the adiabatic approximation, vibronic transitions between different electronic states of the molecule are possible only via coupling to the leads (charging and decharging), and the resulting transport phenomena can be rationalized within the Franck-Condon framework [19,33,49,80,86–90].

Employing an adiabatic basis, nonadiabatic coupling, describing phenomena beyond the Born-Oppenheimer approximation, results from the kinetic-energy operator of the nuclei and would induce additional terms in the Hamiltonian $\sim P_\alpha d_i^\dagger d_j$, where P_α denotes the momentum operator associated with vibrational mode α. As is well known [51,52], however, to describe nonadiabatic coupling phenomena it is often more advantageous to use a so-called diabatic basis, in which the nuclear kinetic-energy operator is (approximately) diagonal and nonadiabatic coupling is described by the nondiagonal elements of the diabatic potential matrix, which (in the linear approximation) are given by the nondiagonal terms $M_{ij}^\alpha Q_\alpha d_i^\dagger d_j$, $i \neq j$ in Eq. (1). This is the electronic basis used in the present paper. Within this diabatic basis, the nondiagonal terms thus represent a breakdown of the adiabatic or Born-Oppenheimer approximation. In the context of nonadiabatic processes in molecules, these terms are often referred to as vibronic coupling [51,52]. Specifically, the molecular Hamiltonian in Eq. (1) corresponds to the well-known vibronic coupling model and describes, e.g., conical intersections of potential-energy surfaces and the associated phenomena [51,52]. In Sec. III we identify the signatures of adiabatic and nonadiabatic coupling mechanisms in charge transport, induced by diagonal and nondiagonal terms of the electronic-vibrational interaction, respectively.

We note in passing that in the context of charge transport the two types of electronic-vibrational coupling discussed above are sometimes also referred to as local or nonlocal coupling [44]. Furthermore, in the case of very strong vibronic coupling, a description based on vibronic many-body eigenstates, which largely abandons the separation between electronic and vibrational degrees of freedom, may be an interesting alternative [91,92].

The left and the right leads of the molecular junction are modeled as macroscopic reservoirs of noninteracting electrons,

$$H_{L/R} = \sum_{k \in L/R} \epsilon_k c_k^\dagger c_k, \tag{2}$$

where ϵ_k is the energy of leads state k and $c_k^\dagger$ and c_k denote the corresponding creation and annihilation operators. The coupling between the electronic states in the molecule and in the leads is described by a tight-binding-like Hamiltonian,

$$H_{ML/MR} = \sum_{k \in L/R, i} V_{ki} c_k^\dagger d_i + \text{H.c.}, \tag{3}$$

with coupling constants V_{ki}.

The Hamiltonian of the overall junction, comprising the molecule and the left and right leads, is given by

$$H = H_{\text{Mol}} + H_L + H_R + H_{ML} + H_{MR}. \tag{4}$$

B. Nonequilibrium Green's function theory

To describe the steady-state transport properties of a molecular junction with electronic-vibrational coupling, we employ the nonequilibrium Green's function approach based on perturbation theory introduced by Kadanoff, Baym, Keldysh, and Langreth [44,85,93–97]. The central objects in describing the nonequilibrium many-body system are the electronic and vibrational Green's functions defined as

$$G_{ij}(\tau, \tau') = -\frac{i}{\hbar} \langle T_c d_i(\tau) d_j^\dagger(\tau') \rangle, \tag{5}$$

$$D_{\alpha\beta}(\tau, \tau') = -\frac{i}{\hbar} \langle T_c Q_\alpha(\tau) Q_\beta(\tau') \rangle. \tag{6}$$

G_{ij} denotes the electronic Green's functions, and i, j label molecular electronic states, whereas $D_{\alpha\beta}$ stands for the vibrational Green's functions and α, β label vibrational modes. T_c is the contour ordering operator in the complex time domain. The Green's functions as well as their retarded and advanced projections obey Dyson's equation, which reads in energy space

$$G_{ij}^{(r/a)}(\epsilon) = G_{ij}^{0(r/a)}(\epsilon) + \sum_{kl} G_{ik}^{0(r/a)}(\epsilon) \Sigma_{kl}^{(r/a)}(\epsilon) G_{lj}^{(r/a)}(\epsilon). \tag{7}$$

The greater and lesser Green's functions satisfy Keldysh's equation

$$G_{ij}^{\lessgtr}(\epsilon) = \sum_{kl} G_{ik}^r(\epsilon) \Sigma_{kl}^{\lessgtr}(\epsilon) G_{lj}^a(\epsilon). \tag{8}$$

$G_{ij}^{0(r/a)}(\epsilon)$ denotes the Green's function of the unperturbed system, without interactions or couplings. k and l label molecular electronic states. $\Sigma_{ij}^{r/a/\langle/\rangle}(\epsilon)$ is the electronic self-energy accounting for the interactions and couplings. In this

model, the self-energy consists of three parts describing the coupling to the left and right leads, respectively, and a part accounting for the electronic-vibrational interaction,

$$\Sigma_{ij}(\epsilon) = \Sigma_{\text{L}\,ij}(\epsilon) + \Sigma_{\text{R}\,ij}(\epsilon) + \Sigma_{\text{vib}\,ij}(\epsilon). \qquad (9)$$

We describe the leads as semi-infinite tight-binding chains with intersite coupling γ [14,65,98]. The self-energies for the coupling to the leads reads

$$\Sigma_{\text{L/R}\,ij}^{r/a}(\epsilon) = \Delta_{\text{L/R}ij}(\epsilon) \mp \frac{\text{i}}{2}\Gamma_{\text{L/R}ij}(\epsilon), \qquad (10)$$

$$\Sigma_{\text{L/R}\,ij}^{<}(\epsilon) = \text{i}\Gamma_{\text{L/R}ij}(\epsilon)f(\epsilon - \mu_{\text{L/R}}), \qquad (11)$$

$$\Sigma_{\text{L/R}\,ij}^{>}(\epsilon) = -\text{i}\Gamma_{\text{L/R}ij}(\epsilon)[1 - f(\epsilon - \mu_{\text{L/R}})]. \qquad (12)$$

Here, $f(\epsilon)$ denotes the Fermi distribution function. The level-width functions $\Gamma_{\text{L/R}\,ij}$ and the level-shift functions $\Delta_{\text{L/R}\,ij}$ have the forms

$$\Gamma_{\text{L/R}ij}(\epsilon) = \frac{V_{\text{L/R}i}V_{\text{L/R}j}^{*}}{\gamma^2}\Theta(4\gamma^2 - x^2)\sqrt{4\gamma^2 - x^2}, \quad (13)$$

$$\Delta_{\text{L/R}ij}(\epsilon) = \frac{V_{\text{L/R}i}V_{\text{L/R}j}^{*}}{2\gamma^2}(x - \Theta(x^2 - 4\gamma^2)\sqrt{x^2 - 4\gamma^2}), \quad (14)$$

respectively, with $x = \epsilon - \mu_{\text{L/R}}$ and the Heaviside step function Θ. We assume that an applied bias voltage leads to a symmetric change in the chemical potentials $\mu_{\text{L/R}} = \pm e\frac{V}{2}$.

We use the standard self-consistent Born approximation (SCBA) to describe the electronic-vibrational interaction [44,74–76,85,96,97,99]. The corresponding self-energy is given by

$$\begin{aligned}\Sigma_{\text{vib}\,ij}^{r}(\epsilon) &= \text{i}\sum_{\substack{k,l\in\text{mol}\\\alpha\in\text{vib}}} M_{ik}^{\alpha}M_{lj}^{\alpha}\int\frac{d\epsilon'}{2\pi}\big[D_{\alpha\alpha}^{0r}(\epsilon-\epsilon')G_{kl}^{r}(\epsilon')\\&\quad + D_{\alpha\alpha}^{0<}(\epsilon-\epsilon')G_{kl}^{r}(\epsilon') + D_{\alpha\alpha}^{0r}(\epsilon-\epsilon')G_{kl}^{<}(\epsilon')\big]\\&\quad - \text{i}\sum_{\substack{k,l\in\text{mol}\\\alpha\in\text{vib}}} M_{ij}^{\alpha}M_{lk}^{\alpha}\int\frac{d\epsilon'}{2\pi}\big[D_{\alpha\alpha}^{0<}(\epsilon=0)G_{kl}^{a}(\epsilon')\\&\quad + D_{\alpha\alpha}^{0r}(\epsilon=0)G_{kl}^{<}(\epsilon')\big],\end{aligned} \qquad (15)$$

$$\Sigma_{\text{vib}\,ij}^{\lessgtr}(\epsilon) = \text{i}\sum_{\substack{k,l\in\text{mol}\\\alpha\in\text{vib}}} M_{ik}^{\alpha}M_{lj}^{\alpha}\int\frac{d\epsilon'}{2\pi}\big[D_{\alpha\alpha}^{0\lessgtr}(\epsilon-\epsilon')G_{kl}^{\lessgtr}(\epsilon')\big]. \qquad (16)$$

The self-energy consists of two parts, the Hartree and the Fock terms. Unlike bulk solid-state systems, the Hartree term, which is given by the terms proportional to $D_{\alpha\alpha}^{0r/<}(\epsilon=0)$ in Eq. (15) and leads to renormalization of the electronic energies, does not vanish since the translational symmetry of the systems under consideration is broken [76,100]. Using Eqs. (7) and (8) and the definition of the self-energy in Eqs. (15) and (16), we obtain a closed set of equations which is solved iteratively.

As the SCBA treats the electronic-vibrational coupling perturbatively, its validity is restricted to the weak-coupling limit. As usual for perturbation theories, a rigorous verification of the validity is often difficult [101]. Studies of the influence

of higher-order processes on transport in nanosystems can be found, for example, in Refs. [102,103]. Furthermore, for simpler models without nonadiabatic coupling, comparisons with numerically exact methods have been used to validate SCBA-type approaches [50]. We also note that under certain conditions, such as strong electronic-vibrational coupling, the SCBA may not give a unique steady-state solution [101]. This is, however, not the case for the weak-coupling parameter regime considered in this work.

The SCBA formalism as outlined above assumes that the vibrational degrees of freedom remain in thermal equilibrium, as indicated by $D_{\alpha\alpha}^{0r/\lessgtr}$. SCBA approaches including nonequilibrium vibrational effects have been used, for example, in Refs. [46,78,99]. Typically, the convergence of the self-consistent cycle including the vibrational degrees of freedom is significantly more demanding, particularly in the resonant transport regime. In the present work, which focuses on the study of basic effects of nonadiabatic coupling on electronic transport properties for model systems, we have therefore restricted the treatment of the vibrational degrees of freedom to equilibrium.

For characterizing the transport properties of a molecular junction, the main observable of interest is the electronic current. It can be calculated using the Meir-Wingreen-like formula [104]

$$I_{\text{L}} = \frac{e}{2\pi\hbar}\sum_{ij}\int[\Sigma_{\text{L}\,ij}^{<}(\epsilon)G_{ji}^{>}(\epsilon) - \Sigma_{\text{L}\,ij}^{>}(\epsilon)G_{ji}^{<}(\epsilon)]d\epsilon. \quad (17)$$

As the SCBA is a current-conserving scheme, i.e., $I_{\text{L}} = -I_{\text{R}}$ holds, it is sufficient to calculate the left current [96,97,105].

The current can be separated, $I_{\text{L}} = I_{\text{L el}} + I_{\text{L inel}}$, into an elastic part $I_{\text{L el}}$ and an inelastic part $I_{\text{L inel}}$ with

$$\begin{aligned}I_{\text{L el}} &= \frac{e}{2\pi\hbar}\sum_{ijkl}\int\big[\Sigma_{\text{L}\,ij}^{<}(\epsilon)G_{jk}^{r}(\epsilon)\Sigma_{\text{R}\,kl}^{>}(\epsilon)G_{li}^{a}(\epsilon)\\&\quad - \Sigma_{\text{L}\,ij}^{>}(\epsilon)G_{jk}^{r}(\epsilon)\Sigma_{\text{R}\,kl}^{<}(\epsilon)G_{li}^{a}(\epsilon)\big]d\epsilon,\end{aligned} \qquad (18)$$

$$\begin{aligned}I_{\text{L inel}} &= \frac{e}{2\pi\hbar}\sum_{ijkl}\int\big[\Sigma_{\text{L}\,ij}^{<}(\epsilon)G_{jk}^{r}(\epsilon)\Sigma_{\text{vib}\,kl}^{>}(\epsilon)G_{li}^{a}(\epsilon)\\&\quad - \Sigma_{\text{L}\,ij}^{>}(\epsilon)G_{jk}^{r}(\epsilon)\Sigma_{\text{vib}\,kl}^{<}(\epsilon)G_{li}^{a}(\epsilon)\big]d\epsilon.\end{aligned} \qquad (19)$$

Following [14,99], applying Dyson's equation (7), the elastic current can be split into an electronic part and elastic correction part with

$$\begin{aligned}I_{\text{L el}}^{0} &= \frac{e}{2\pi\hbar}\sum_{ijkl}\int\big[\Sigma_{\text{L}\,ij}^{<}(\epsilon)G_{jk}^{0r}(\epsilon)\Sigma_{\text{R}\,kl}^{>}(\epsilon)G_{li}^{0a}(\epsilon)\\&\quad - \Sigma_{\text{L}\,ij}^{>}(\epsilon)G_{jk}^{0r}(\epsilon)\Sigma_{\text{R}\,kl}^{<}(\epsilon)G_{li}^{0a}(\epsilon)\big]d\epsilon,\end{aligned} \qquad (20)$$

$$\delta I_{\text{L el}} = I_{\text{L el}} - I_{\text{L el}}^{0}. \qquad (21)$$

$I_{\text{L el}}^{0}$ is the electronic current, which is the current in the absence of electronic-vibrational interactions. $\delta I_{\text{L el}}$ is the elastic correction introduced by the electronic-vibrational coupling. In the lowest order, this contribution is proportional to $\Sigma_{\text{vib}\,ij}^{0r/a}(\epsilon)$ and describes processes including the emission and reabsorption of virtual vibrational quanta [14,106].

C. Nonequilibrium Green's function theory and interference effects

The Green's function approach offers a description of the electronic transport including quantum coherences. Therefore, it accounts for interference effects between different transport channels, which have received significant attention recently [30,31,107]. Thereby, different approaches have been used for analysis, including the use of the eigenbasis of the molecular subspace [30,108] or transformations to conducting orbitals [109]. In this work, we apply the approach used in Ref. [33] to identify interference effects in transport, which employs the basis of molecular states to express the transmission function

$$T(\epsilon) = \sum_{ij} \Gamma_{Lij}(\epsilon) G_{ji}^{>}(\epsilon). \tag{22}$$

Within this framework, the incoherent contribution to transport is obtained by neglecting the off-diagonal parts of the self-energy of the coupling to the left lead,

$$T_{\text{incoh}}(\epsilon) = \sum_{i} \Gamma_{Lii}(\epsilon) G_{ii}^{>}(\epsilon). \tag{23}$$

This corresponds to a coupling of the electronic states to separate electrodes, excluding the effect of interference. Accordingly, the part of the transmission function describing interference effects reads

$$T_{\text{interf}}(\epsilon) = T(\epsilon) - T_{\text{incoh}}(\epsilon) = \sum_{i,j\neq i} \Gamma_{Lij}(\epsilon) G_{ji}^{>}(\epsilon). \tag{24}$$

III. RESULTS

In this section, we analyze the influence of nonadiabatic electronic-vibrational coupling on the transport properties of model systems. The parameters characterizing the model systems, summarized in Table I, represent typical values for molecular junctions. The electronic-vibrational interaction strengths have been chosen in the weak-coupling regime such that the SCBA is expected to be valid.

This section is separated into two parts, depending on the energy spacing between the electronic levels. In Sec. III A we discuss the effect of electronic-vibrational coupling for two-level systems with well-separated electronic states, including an analytic study of important vibrational effects in Sec. III A 1, a comparison of the influence of adiabatic and nonadiabatic vibrational interactions in Sec. III A 2, and an investigation of the transport properties of model systems with increased complexity in Secs. III A 2–III A 4. In Sec. III B, we study the influence of electronic-vibrational interactions in two-level systems with quasidegenerate electronic levels. For such systems, quantum interference effects are important and sensitive to the electronic-vibrational interaction [26,28,30,31,33].

A. Transport properties of molecular conductors with well-separated electronic states

In this section we investigate the effect of nonadiabatic electronic-vibrational coupling on the transport properties of molecular junctions with well-separated electronic levels, i.e., with energy spacings that exceed their broadening induced by the coupling to the leads. For the sake of clarity, we restrict our discussion to systems with a single vibrational mode, dropping the vibrational indices. A generalization to multimode systems is, in principle, straightforward.

1. Identification of dominant processes

We first analyze the current as the main transport observable. Since the method outlined in Sec. II B restricts the investigation to model systems where perturbation theory is valid, we perform an expansion of the current in M_{ij} and V_{ij} to lowest nonvanishing order. This allows us to systematically identify the most important transport processes.

To this end, we introduce the shorthand notations

$$\mathcal{G}_{ij}^{r}(\epsilon) = i \int \frac{d\epsilon'}{2\pi} \big[D^{0r}(\epsilon - \epsilon') G_{ij}^{r}(\epsilon') + D^{0<}(\epsilon - \epsilon') G_{ij}^{r}(\epsilon') + D^{0r}(\epsilon - \epsilon') G_{ij}^{<}(\epsilon') \big], \tag{25}$$

$$\mathcal{G}_{ij}^{\lessgtr}(\epsilon) = i \sum_{kl} \int \frac{d\epsilon'}{2\pi} \big[D^{0\lessgtr}(\epsilon - \epsilon') G_{ik}^{r}(\epsilon') \Sigma_{kl}^{\lessgtr}(\epsilon') G_{lj}^{a}(\epsilon') \big], \tag{26}$$

which appear in the definition of the vibrational self-energies (15) and (16). A lowest-order estimate of $\mathcal{G}_{ij}^{r\lessgtr}(\epsilon)$ can be obtained by inserting the expressions for free-particle Green's functions into the right-hand sides of Eqs. (25) and (26). We identify $\mathcal{G}_{ij}^{0r}(\epsilon) \triangleq G_{ij}^{0r}(\epsilon - \hbar\Omega)$ and $\mathcal{G}_{ij}^{0\lessgtr}(\epsilon) \triangleq G_{ij}^{0\lessgtr}(\epsilon - \hbar\Omega)$ in this order.

Vibrational effects in the current appear in the elastic corrections (21) and the inelastic current (19). For weak coupling, the most important vibrational effects are of lowest nonvanishing order in the electronic-vibrational and the molecule-lead coupling, $O(M^2 V^4)$. To this order and for low

TABLE I. Parameters describing the model systems investigated in this paper. For all calculations, the temperature is $T = 10$ K. All parameters are given in eV.

Model	ϵ_1	ϵ_2	V_{L1}	V_{R1}	V_{L2}	V_{R2}	γ	$\hbar\Omega$	M_{11}	M_{22}	M_{12}
AD	0.25	0.4	0.1	0.1	0.1	0.1	3	0.025–0.3	0.03	0.03	0.0
NONAD	0.25	0.4	0.1	0.1	0.1	0.1	3	0.025–0.3	0.0	0.0	0.03
ASYMM	0.25	0.4	0.02	0.2	0.2	0.02	3	0.1	0.0	0.0	0.03
INTPLY	0.25	0.4	0.1	0.1	0.1	0.1	3	0.1	0.02, 0.05	0.02, 0.05	0.0, ±0.02, 0.05
DESNONAD	0.5	0.3–0.7	0.1	0.1	0.1	−0.1	2	0.1			0, 0.05
DESVIB	0.5	0.505	0.1	0.1	0.1	−0.1	2	0.1	0.0	0.05	0.0–0.02
DES	0.5	0.505	0.1	0.1	0.1	−0.1	2				

temperature, the parts of the current influenced by the vibrations read

$$\delta I_{\mathrm{L\,el}} = \frac{e}{2\pi\hbar}\sum_{ijklm}\int \left\{\Sigma^{<}_{\mathrm{L}\,ij}(\epsilon)[G^{0r}_{jj}(\epsilon)M_{jl}M_{mk}\mathcal{G}^{0r}_{lm}(\epsilon)G^{0r}_{kk}(\epsilon)G^{0a}_{ii}(\epsilon) + \mathrm{H.c.}]\Sigma^{>}_{\mathrm{R}\,ki}(\epsilon)\right\}d\epsilon$$

$$-\frac{e}{2\pi\hbar}\sum_{ijkl}\int\left[\Sigma^{<}_{\mathrm{L}\,ij}(\epsilon)\left(G^{0r}_{jj}(\epsilon)M_{jl}M_{lk}\frac{2n_{ll}}{\hbar\Omega}G^{0r}_{kk}(\epsilon)G^{0a}_{ii}(\epsilon) + \mathrm{H.c.}\right)\Sigma^{>}_{\mathrm{R}\,ki}(\epsilon)\right]d\epsilon + O(M^4V^6), \tag{27}$$

$$I_{\mathrm{L\,inel}} = \frac{e}{2\pi\hbar}\sum_{ijkl}\int\left[\Sigma^{<}_{\mathrm{L}\,ji}(\epsilon)G^{0r}_{ii}(\epsilon)M_{ik}M_{lj}\mathcal{G}^{0>}_{kl}(\epsilon)G^{0a}_{jj}(\epsilon)\right]d\epsilon + O(M^4V^6), \tag{28}$$

where n_{ll} denotes the population of the electronic state l. This expression can be further simplified for well-separated electronic levels. Under this assumption, the product of two Green's functions at the same energy but for different electronic states is negligible. Note that this approximation does not rely on perturbation theory and uses the fact that the electronic Green's functions are strongly peaked at their resonances. Applying this simplification, Eqs. (27) and (28) reduce to

$$\delta I_{\mathrm{L\,el}} \approx \frac{e}{2\pi\hbar}\sum_i\left(\int \Sigma^{<}_{\mathrm{L}\,ii}(\epsilon)\left\{|G^{0r}_{ii}(\epsilon)|^2 G^{0r}_{ii}(\epsilon)\left[M^2_{ii}\mathcal{G}^{0r}_{ii}(\epsilon) + \sum_{j\neq i}|M_{ij}|^2\mathcal{G}^{0r}_{jj}(\epsilon)\right] + \mathrm{H.c.}\right\}\Sigma^{>}_{\mathrm{R}\,ii}(\epsilon)\right.$$

$$\left. - \Sigma^{<}_{\mathrm{L}\,ii}(\epsilon)\left\{|G^{0r}_{ii}(\epsilon)|^2 G^{0r}_{ii}(\epsilon)\frac{2}{\hbar\Omega}\left[M^2_{ii}n_{ii} + \sum_{j\neq i}|M_{ij}|^2 n_{jj}\right] + \mathrm{H.c.}\right\}\Sigma^{>}_{\mathrm{R}\,ii}(\epsilon)d\epsilon\right) + O(M^4V^6), \tag{29}$$

$$I_{\mathrm{L\,inel}} \approx \frac{e}{2\pi\hbar}\sum_i\int \Sigma^{<}_{\mathrm{L}\,ii}(\epsilon)|G^{0r}_{ii}(\epsilon)|^2\left[M^2_{ii}\mathcal{G}^{0>}_{ii}(\epsilon) + \sum_{j\neq i}|M_{ij}|^2\mathcal{G}^{0>}_{jj}(\epsilon)\right]d\epsilon + O(M^4V^6). \tag{30}$$

The influence of the vibrations on the current separates into two parts. The first one, proportional to $M^2_{ii}\mathcal{G}^{0r/>}_{ii}(\epsilon)$, depends only on the adiabatic electronic-vibrational coupling. The second part is proportional to $|M_{ij}|^2\mathcal{G}^{0r/>}_{jj}(\epsilon)$ with $j \neq i$ and depends only on the nonadiabatic coupling strengths. Although the analytic description of these terms is analogous to the purely adiabatic terms, the nonadiabatic processes depend on two different electronic levels leading to a distinct dependence on the energies ϵ_i, ϵ_j, and $\hbar\Omega$, which will be exemplified in the following sections. Pronounced nonadiabatic vibrational effects appear if the resonance condition $\epsilon_i \approx \epsilon_j + \hbar\Omega$ is satisfied. This behavior is qualitatively different from the Franck-Condon picture for adiabatic electronic-vibrational effects. Accordingly, the adiabatic approximations is valid as long as the nonadiabatic coupling strengths M_{ij} are small and the resonance condition is not fullfiled for any pair of the electronic states i and j. This is reminiscent of the validity of the Born-Oppenheimer approximation. Notice that beyond the lowest-order approximation in the molecule-lead coupling, the exact form of the level broadening provided by the leads influences the impact of the individual vibrational effects. Since in Eqs. (29) and (30) the electronic-vibrational coupling decomposes into a purely adiabatic part and a purely nonadiabatic part, we start the model-based investigation of the nonadiabatic electronic-vibrational coupling below by a comparison between the well-known adiabatic effects and the influence of purely nonadiabatic electronic-vibrational couplings in Secs. III A 2 and III A 3.

Neglecting the product between two Green's functions at the same energy but for different electronic states is an approximation, which does not hold, for example, in systems where the coupling to the leads allows for strong mixing between the different electronic states, resulting in large off-diagonal components of the self-energy for the leads.

In the Appendix, we go beyond this approximation and analyze higher-order processes as well as the interplay between adiabatic and nonadiabatic electronic-vibrational interactions. The latter is of importance for Sec. III A 4.

2. Comparison between adiabatic and nonadiabatic electronic-vibrational couplings

To analyze the mechanisms and signatures of adiabatic and nonadiabatic electronic-vibrational couplings, we first consider the two effects separately. To this end, we compare results for two models subject to nonadiabatic electronic-vibrational coupling (labeled NONAD; $M_{ii} = 0$) and adiabatic electronic-vibrational coupling (labeled AD; $M_{ij} = 0$ for $i \neq j$), respectively. The parameters defining these model systems are given in Table I.

Figure 1 shows the current-voltage characteristics for the model systems AD and NONAD for two different vibrational energies $\hbar\Omega = 0.025$ eV and $\hbar\Omega = 0.14$ eV. The vibrational energies are chosen such that significant adiabatic ($\hbar\Omega = 0.025$ eV) and nonadiabatic vibrational effects ($\hbar\Omega = 0.14$ eV) can be observed. A more comprehensive comparison between adiabatic and nonadiabatic electronic-vibrational effects is provided by the conductance map in Fig. 2, which depicts the conductance $\frac{\partial I}{\partial V}$ as a function of voltage and vibrational energy $\hbar\Omega$.

For both models, the current-voltage characteristics are dominated by two steps at different voltages which lead to lines in the conductance maps. These features correspond to the onset of resonant transport through the electronic states as depicted in Fig. 3(a) for the lower electronic state. The position of the steps is determined by the energies of the electronic states renormalized by the coupling to the vibrations $\bar{\epsilon}_{1/2}$. In the purely adiabatic case, this renormalization is described by the polaron shift [19,84,85] (black dashed lines in the
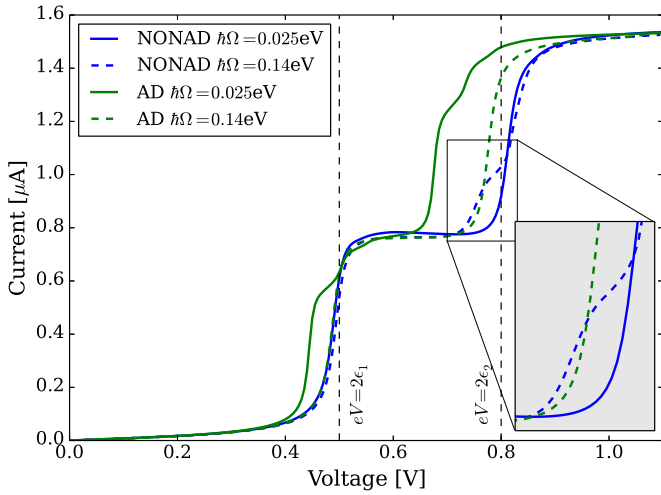
FIG. 1. (Color online) Current-voltage characteristics of two molecular junctions described by the models AD and NONAD for two different vibrational energies. The onset of resonant transport through the electronic levels in the absence of vibrations is marked by vertical dashed lines. The inset provides a close-up of a region relevant for nonadiabatic vibrational effects.

conductance map of AD in Fig. 2). The electronic resonances of the model NONAD, on the other hand, coincide very well with the unperturbed energies $\epsilon_{1/2}$ (black dashed lines in the conductance map of NONAD in Fig. 2). As the purely nonadiabatic electronic-vibrational interaction provides a coupling between the electronic states, the energy shift due to the vibrations depends on the energy difference between the electronic states (for details see Sec. III B 1). The levels in NONAD are well separated; therefore, the electronic energies are almost unchanged.
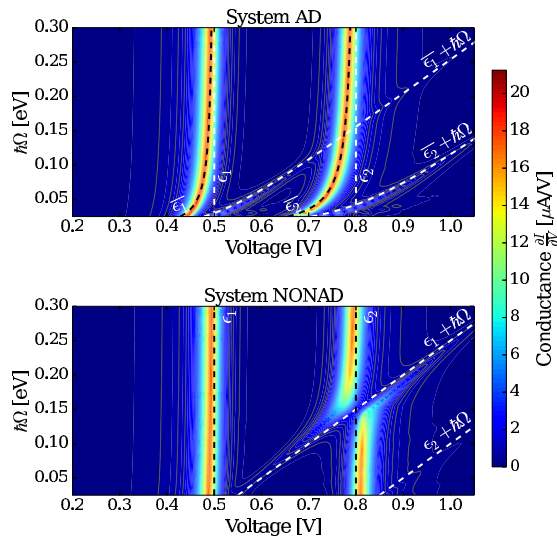
FIG. 2. (Color online) Conductance map for the model systems (top) AD and (bottom) NONAD. In both plots, the conductance $\frac{\partial I}{\partial V}$ is plotted as a function of voltage V and and vibrational energy $\hbar\Omega$. The dashed lines indicate the positions of the unperturbed electronic resonances $\epsilon_{1/2}$, the electronic resonances renormalized by the coupling to the vibrations $\bar{\epsilon}_{1/2}$ as well as their respective vibrational satellites.

Apart from the electronic resonances, the current exhibits additional smaller steps and the conductance exhibits additional, less pronounced lines at $eV = 2(\bar{\epsilon}_{1/2} + n\hbar\Omega)$ ($n \in \mathbf{N}$; white dashed lines in the conductance maps in Fig. 2). Notice that vibrational features are clearly visible only for $n = 1$ since the SCBA is restricted to weak electronic-vibrational coupling. For the system AD, these features are more pronounced for small $\hbar\Omega$ (which results in a stronger dimensionless coupling $\frac{M_{ii}}{\hbar\Omega}$), whereas for the system NONAD they are present only for vibrational energies close to the resonance condition $\epsilon_1 + \hbar\Omega = \epsilon_2$. In this region, the conductance map of NONAD also exhibits an avoided level crossing (intersection between white dashed line and black dashed line in Fig. 2, bottom). These features correspond to the onset of transport processes, where electrons populate the molecular bridge resonantly upon the excitation of n vibrational quanta. Examples of such processes are shown in Figs. 3(b)–3(e).

It was shown that the step height corresponding to adiabatic vibronic processes can be described by the Franck-Condon factors and depends only on the dimensionless coupling $M_{ii}/\hbar\Omega$. As the processes include only one electronic level, the broadening of the electronic level and its proximity to its vibrational satellites are important for pronounced adiabatic vibrational effects in the current [see color coding in Figs. 3(b) and 3(d)].

Nonadiabatic electronic-vibrational processes, on the other hand, include two different electronic states. In this process, depicted in Fig. 3(c), one electronic state is populated from the left lead, whereas the other state allows the electron to leave the molecule towards the right lead. The intramolecular transition between the electronic states is facilitated by the coupling to the vibrations, and the energy of the electron is changed by $\hbar\Omega$. The probability for this nonadiabatic process is enhanced if the resonance condition $\epsilon_1 + \hbar\Omega = \epsilon_2$ is fulfilled [57]. Because the system NONAD comprises only a single vibrational degree of freedom, the nonadiabatic transport process results in an avoided level crossing as a signature of the breakdown of the Born-Oppenheimer approximation. In systems with more vibrational degrees of freedom, true degeneracies are also possible, for example, in systems with a conical intersection of potential-energy surfaces [52].

3. Transport channels due to nonadiabatic electronic-vibrational coupling and asymmetric current-voltage characteristics

As shown, nonadiabatic electronic-vibrational coupling provides a mechanism that mixes the electronic levels of the molecular bridge even without coupling to the leads. This induces additional transport channels, which are not available within the adiabatic approximation. A particular interesting scenario arises in junctions with asymmetric, state-specific coupling to the leads. As an example, we consider the model ASYMM, where the lower electronic state couples strongly to the right lead and weakly to the left, whereas the other electronic level is strongly coupled to the left lead and weakly to the right. The corresponding parameters can be found in Table I. A system with similar coupling to the leads but without nonadiabatic electronic-vibrational coupling was investigated in [49].

Figure 4 depicts the current-voltage characteristic of the model ASYMM with and without electronic-vibrational
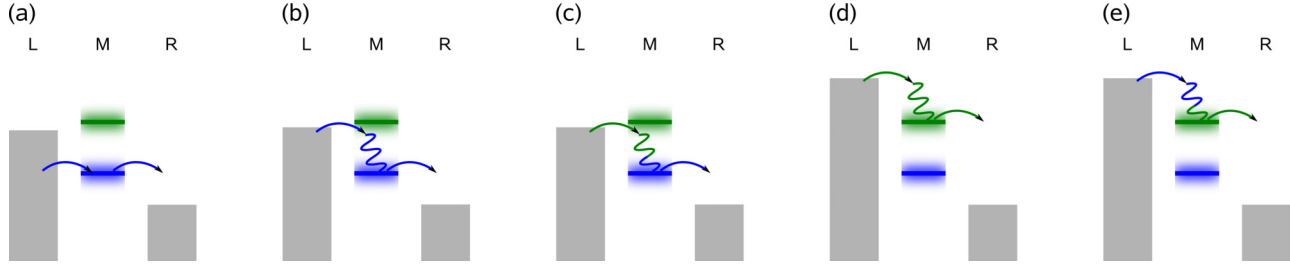
FIG. 3. (Color online) Schematic representation of example processes for (a) purely electronic and (b)–(e) vibronic transport involving the emission of one vibrational quantum and two broadened electronic levels. The abbreviations L and R denote the left and the right leads, respectively, and M stands for the molecule. The arrows illustrate tunneling electrons, whereas the color of the arrow denotes the molecular level involved in the tunneling process.

coupling. While the noninteracting model shows only a small current, the model with finite electronic-vibrational coupling, $M_{12} = 0.03$ eV, is a far better conductor with a pronounced inelastic current. As is well known, the current-voltage characteristics for the noninteracting model is, despite the asymmetry of the molecule lead coupling, symmetric with respect to bias polarity [44,110]. The nonadiabatic vibrational coupling, however, results in a pronounced asymmetry of the current-voltage characteristics. The inelastic currents obtained for positive and negative bias polarities differ not only in magnitude but also with respect to the voltages at which steps in the current appear.

This is due to the fact that nonadiabatic electronic-vibrational interaction provides additional inelastic transport channels described by the expressions

$$I_{ij} = \frac{e}{2\pi\hbar} \int \Sigma^{<}_{L\,ii}(\epsilon) \left| G^r_{ii}(\epsilon) \right|^2 |M_{ij}|^2 \mathcal{G}^{>}_{jj}(\epsilon) d\epsilon$$

$$= \frac{e}{2\pi\hbar} \int \Sigma^{<}_{L\,ii}(\epsilon) \left| G^{0r}_{ii}(\epsilon) \right|^2 |M_{ij}|^2 \left| G^{0r}_{jj}(\epsilon - \hbar\Omega) \right|^2$$

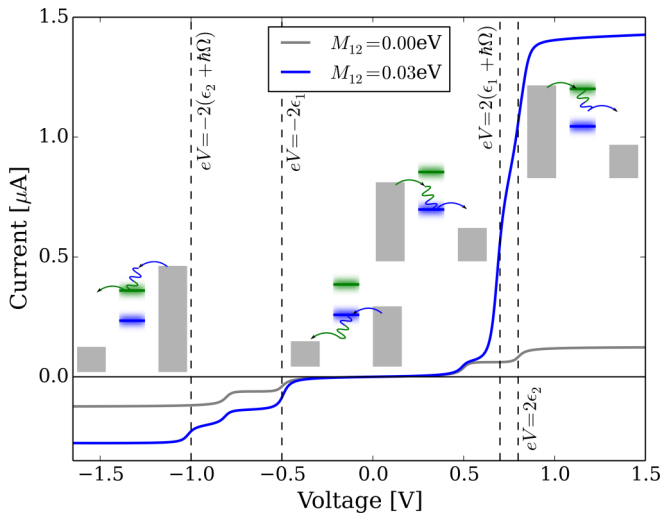$$\times \Sigma^{>}_{R\,jj}(\epsilon - \hbar\Omega) d\epsilon + O(M^4 V^6) \qquad (31)$$

FIG. 4. (Color online) Current-voltage characteristics for the system ASYMM. The pictures given in this plot visualize the most important vibrational transport processes. The vertical dashed lines mark the voltages at which relevant unperturbed electronic energy levels enter the voltage window.

for the current with $i, j \in \{1,2\}$, $i \neq j$. The additional steps in the inelastic current correspond to resonant transport processes depicted in Fig. 4.

As the molecule couples asymmetrically to the leads, transport is dominated by inelastic channels that can exploit the strong couplings of the higher molecular electronic level to the left lead and of the lower molecular electronic level to the right lead. The transition between the electronic states is enabled by the interaction with the vibrations, where electrons scatter from the higher to the lower electronic level, thereby exciting the vibrational mode. Due to the low temperature of $T = 10$ K, the reverse process including the absorption of vibrational energy is strongly suppressed. For positive bias voltage, the asymmetric coupling to the leads together with the energetic restriction imposed by the emission of vibrational quanta results in a pronounced inelastic current that profits from the energetic proximity of $\epsilon_1 + \hbar\Omega$ and ϵ_2. For negative bias, on the other hand, the necessity to emit vibrational energy restricts the system to different inelastic transport processes, which do not benefit from the resonance condition found in Sec. III A 1. This leads to a smaller current which exhibits steps at different voltages.

This example shows that nonadiabatic electronic-vibrational coupling in junctions with asymmetric, state-specific molecule-lead coupling may result in a pronounced asymmetry of the current, i.e., a rectification effect. It is noted that vibrationally induced rectification is also observed in similar models with adiabatic electronic-vibrational coupling [19,90]; the underlying mechanism, however, is quite different.

4. Interplay between adiabatic and nonadiabatic electronic-vibrational couplings

In real-world molecules, both the adiabatic and nonadiabatic electronic-vibrational interactions will be active and will influence the transport properties in a more complex way than in the simplified models discussed above. The dominating contributions to the current from the adiabatic and nonadiabatic coupling mechanisms and their interplay in this more general scenario are analyzed in the Appendix. As an illustrative example, we consider the model INTPLY, with parameters as specified in Table I.

We first consider in Fig. 5 a model system which is dominated by the adiabatic coupling $M_{11} = M_{22} = 0.05$ eV but exhibits, in addition, a smaller nonadiabatic coupling $M_{12} = \pm 0.02$ eV. The results reveal a significant influence of the nonadiabatic coupling in the voltage range between $eV =$
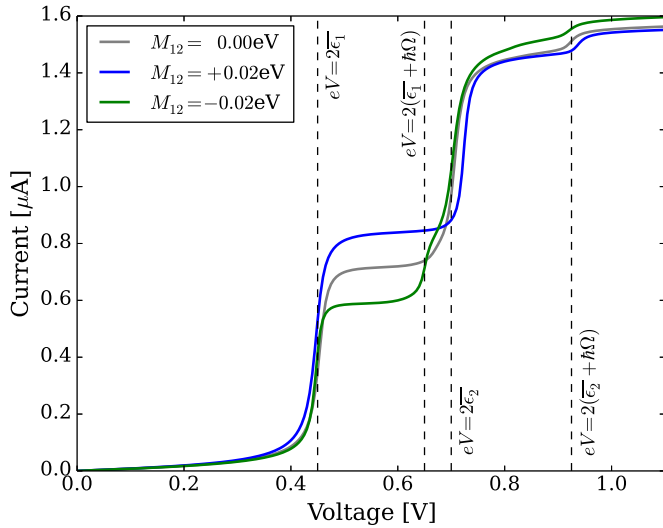
FIG. 5. (Color online) Current-voltage characteristics for the model system INTPLY for $M_{11}, M_{22} = 0.05$ eV and $M_{12} = 0, \pm 0.02$ eV. The vertical dashed lines denote the voltages at which resonant transport through the molecular states, renormalized by the adiabatic electronic-vibrational coupling, becomes possible.

$2\overline{\epsilon}_1$ and $eV = 2(\overline{\epsilon}_1 + \hbar\Omega)$, where $\overline{\epsilon}_1 = \epsilon_1 - \frac{M_{11}^2}{\hbar\Omega}$ denotes the energy of the first electronic state renormalized by the adiabatic coupling to the vibrations (polaron shift). In particular, the current depends on the sign of the nonadiabatic coupling M_{12}.

To analyze the underlying mechanism, in Fig. 6 we separate the current into incoherent and interference parts, according to Eqs. (23) and (24). The results show that the change of the current induced by nonadiabatic coupling can be considered as an interference effect, whereby positive (negative) coupling M_{12} results in constructive (destructive) interference. Because the electronic levels of the system INTPLY are well separated, the effect occurring in the voltage range between $eV = 2\overline{\epsilon}_1$ and $eV = 2(\overline{\epsilon}_1 + \hbar\Omega)$ cannot be caused by interference of pathways associated with different electronic states. As is analyzed
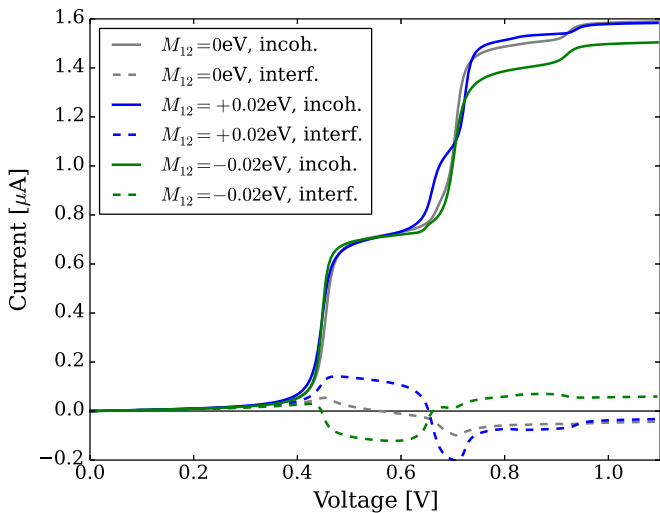

FIG. 6. (Color online) Interference (dashed lines) and incoherent (solid lines) contributions to the currents of the system INTPLY for $M_{11}, M_{22} = 0.05$ eV and $M_{12} = 0, \pm 0.02$ eV depicted in Fig. 5.
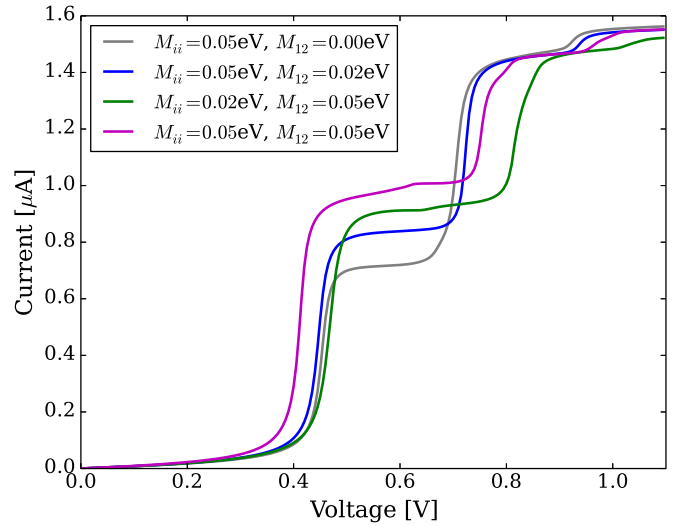

FIG. 7. (Color online) Current-voltage characteristics for the model system INTPLY. The electronic-vibrational coupling parameters are specified in the legend.

in more detail in the Appendix, it rather corresponds to the interference of different vibronic contributions to the current induced by adiabatic and nonadiabatic electronic-vibrational couplings [see. Eqs. (A1) and (A2)]. Thus, currents from adiabatic and nonadiabatic electronic-vibrational processes interfere with each other. For higher voltages, when the second electronic state enters the bias window, the effect disappears. This is because the self-energy for the coupling to the leads gives off-diagonal Green's function elements that differ in sign for the states $\epsilon_{1/2}$. As a result, transport processes where the role of the electronic states is interchanged contribute with opposite signs to the overall current and thus cancel each other.

It is also noted that the interplay between adiabatic and nonadiabatic electronic-vibrational coupling breaks the symmetry of the current with respect to the first and second electronic states: Without nonadiabatic coupling, the transport through the two electronic levels contributes approximately equally to the current (for a system with the same molecule-lead and vibronic couplings for the two states as considered here and neglecting nonequilibrium vibrational effects and electron-electron interactions). For a system with additional nonadiabatic coupling, the increase in the current at the bias voltages $eV = 2\overline{\epsilon}_1$ and $eV = 2\overline{\epsilon}_2$ differs due to the interference between nonadiabatic and adiabatic contributions, as discussed above.

Next, we analyze the influence of the relative strength of the adiabatic M_{ii} and nonadiabatic M_{ij} electronic-vibrational coupling. To this end, Fig. 7 depicts the current-voltage characteristics of the system INTPLY for several scenarios: the case with only adiabatic coupling ($M_{ii} = 0.05$ eV, $M_{12} = 0$ eV), the cases where adiabatic coupling ($M_{ii} = 0.05$ eV, $M_{12} = 0.02$ eV) and nonadiabatic coupling ($M_{ii} = 0.02$ eV, $M_{12} = 0.05$ eV) are dominant, and also the case where adiabatic and nonadiabatic couplings are of the same strength ($M_{ii} = M_{12} = 0.05$ eV). The results reveal a significant dependence of the magnitude of the current and the location of the steplike structures in the current on the relative coupling strengths M_{ii} and M_{ij}.

The different bias voltages at which the steplike increase of the current is observed can be rationalized by the different energy-level renormalization caused by adiabatic and nonadiabatic electronic-vibrational couplings, respectively. The adiabatic coupling leads to a decrease in the energy of all the electronic levels described by the polaron shift. The nonadiabatic interaction, on the other hand, results in a repulsion of the electronic levels.

The difference of the level of the currents, observed in Fig. 7 for voltages between 0.4 and 0.7 V, can again be identified as an interference effect according to Eqs. (23) and (24), like in the discussion above. The first estimate provided by Eqs. (A1) and (A2) suggests that the different contributions to the current are proportional to the product of adiabatic and nonadiabatic coupling strengths $M_{ii}M_{jk}$. This explains the enhanced current of the model with $M_{ii} = 0.05$ eV and $M_{12} = 0.02$ eV compared to that of the purely adiabatic model and also why the model system with $M_{ii} = 0.05$ eV and $M_{12} = 0.05$ eV exhibits the largest current. The deviations between the models with couplings $M_{ii} = 0.02$ eV, $M_{12} = 0.05$ eV and $M_{ii} = 0.05$ eV, $M_{12} = 0.02$ eV, on the other hand, indicate a difference between adiabatic and nonadiabatic couplings which is beyond the level of approximation discussed in the Appendix.

B. Transport properties of molecular junctions with quasidegenerate electronic states

In this section we investigate the effect of nonadiabatic electronic-vibrational coupling on model systems with quasidegenerate electronic levels. We refer to molecular states as quasidegenerate whenever the energy difference between the states is smaller than the level broadening due to coupling to the leads. For such a model system, quantum interference plays an important role, and adiabatic electronic-vibrational coupling has been shown to result in decoherence effects [26,28,30,31,33].

1. Electronic two-level system with constant interstate coupling

The identification of dominant transport processes for systems with quasidegenerate electronic states in analogy to the approach in Sec. III A 1 is significantly more involved than for well-separated energy levels. To analyze their transport properties, we therefore consider a simplified toy model consisting of two electronic levels with constant coupling between the two electronic states at the molecular bridge instead of the vibronic coupling described by Eq. (1).

$$H' = \epsilon_1 d_1^\dagger d_1 + \epsilon_2 d_2^\dagger d_2 + \Delta(d_1^\dagger d_2 + d_2^\dagger d_1) + \sum_{k \in \text{L/R}} \epsilon_k c_k^\dagger c_k$$
$$+ \sum_{k \in \text{L/R}} (V_{k1} c_k^\dagger d_1 + V_{k2} c_k^\dagger d_2 + \text{H.c.}), \quad (32)$$

where Δ is the constant interstate coupling strength. The part of the Hamiltonian without the coupling to the leads can be diagonalized by a simple basis transformation, resulting in

$$H' = \tilde{\epsilon}_1 \tilde{d}_1^\dagger \tilde{d}_1 + \tilde{\epsilon}_2 \tilde{d}_2^\dagger \tilde{d}_2 + \sum_{k \in \text{L/R}} \epsilon_k c_k^\dagger c_k$$
$$+ \sum_{k \in \text{L/R}} (\tilde{V}_{k1} c_k^\dagger \tilde{d}_1 + \tilde{V}_{k2} c_k^\dagger \tilde{d}_2 + \text{H.c.}). \quad (33)$$

Here, $\tilde{d}_i^\dagger$ and $\tilde{d}_i$ are the fermionic creation and annihilation operators in the new basis. The new energies $\tilde{\epsilon}_{1/2}$ and couplings to the leads $\tilde{V}_{k1/2}$ are given by

$$\tilde{\epsilon}_{1/2} = \frac{\epsilon_1 + \epsilon_2}{2} \pm \sqrt{\left(\frac{\epsilon_2 - \epsilon_1}{2}\right)^2 + \Delta^2}, \quad (34)$$

$$\tilde{V}_{k1/2} = \frac{N_{1/2}}{\tilde{\epsilon}_2 - \tilde{\epsilon}_1} \left(\pm \frac{\tilde{\epsilon}_{2/1} - \epsilon_1}{\Delta} V_{k1} \mp V_{k2}\right), \quad (35)$$

where the shorthand notation $N_{1/2} = \sqrt{\Delta^2 + (\epsilon_1 - \tilde{\epsilon}_{1/2})^2}$ was used.

For the model systems considered in Secs. III B 2 and III B 3, $V_{k1} = \pm V_{k2}$ holds. In this case, upon increasing Δ, one of the new electronic states couples more strongly to the left and more weakly to the right lead, whereas the other electronic state couples more strongly to the right and more weakly to the left lead. This results in a decreasing conductivity of the model system with increasing coupling strength Δ or decreasing level spacing $|\epsilon_2 - \epsilon_1|$. In the limit $\Delta \to \infty$ or $|\epsilon_2 - \epsilon_1| \to 0$, the system decomposes into a state coupling only to the left lead and another state coupling only to the right lead, such that the current flowing through the molecule vanishes.

2. Influence of purely nonadiabatic electronic-vibrational interactions

We first consider transport through a molecular system exhibiting quasidegenerate electronic states with a purely nonadiabatic electronic-vibrational coupling. This scenario is described by the model system DESNONAD with parameters specified in Table I. It is noted that the model DESNONAD is analogous to the model system DES studied by Härtle *et al.* [33] but extended by the nonadiabatic electronic-vibrational coupling. The system without electronic-vibrational coupling is known to exhibit strong destructive interference effects which suppress the current. Therefore, the model system allows for a systematic investigation of the influence of purely nonadiabatic electronic-vibrational interactions on interferences.

An example of a typical current-voltage characteristic for the system DESNONAD with electronic energy $\epsilon_2 = 0.505$ eV is given in Fig. 8, where the current for the system with nonadiabatic electronic-vibrational coupling $M_{12} = 0.05$ eV is compared to that without electronic-vibrational coupling. The energy difference between the electronic states plays a crucial role for the interference effects. A more systematic investigation of the model system DESNONAD can therefore be obtained by studying the transport properties as a function of the electronic energy ϵ_2 while keeping all other parameters fixed, as done in the conductance map in Fig. 9.

Figure 8 shows that the current for the interacting system is significantly smaller than that for the noninteracting system. Furthermore, it exhibits two resonance steps instead of one. The more detailed conductance map shows two distinguishable resonances for any value of ϵ_2, and an avoided level crossing as well as vanishing conductance for $\epsilon_2 = \epsilon_1$. Furthermore, negative differential resistances (NDRs), that is, a decrease in the current upon an increase in the bias voltage, are observed close to the line $\epsilon_2 = \epsilon_1$ for bias voltages when the second
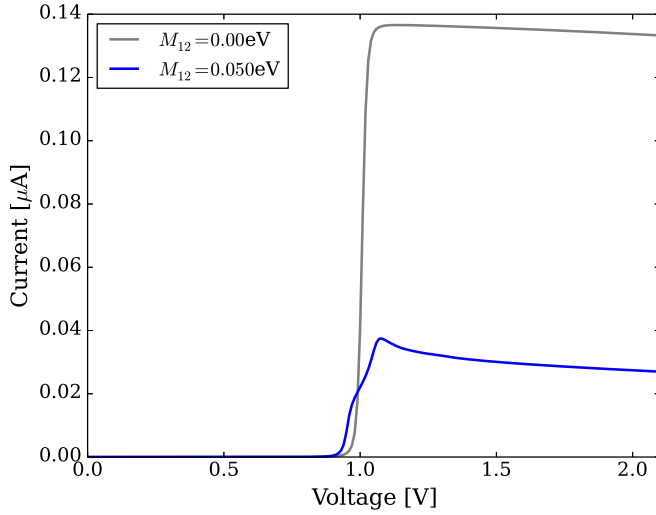
FIG. 8. (Color online) Current-voltage characteristics of the system DESNONAD for $\epsilon_2 = 0.505$ eV with and without nonadiabatic electronic-vibrational coupling.

electronic resonance enters the bias window. Apart from that, the conductance map shows two additional avoided level crossings for $\epsilon_2 + \hbar\Omega = \epsilon_1$ and $\epsilon_1 + \hbar\Omega = \epsilon_2$ (intersection of white dashed lines). This last effect has already been discussed in Sec. III A 2 and will not be further addressed here.

To rationalize these findings, we consider the simplified noninteracting model system with constant interstate coupling from Sec. III B 1. A coupling between the electronic states of the molecule leads to a renormalization of the electronic energies and therefore to an avoided level crossing, resulting in two steps in the corresponding current. To a good
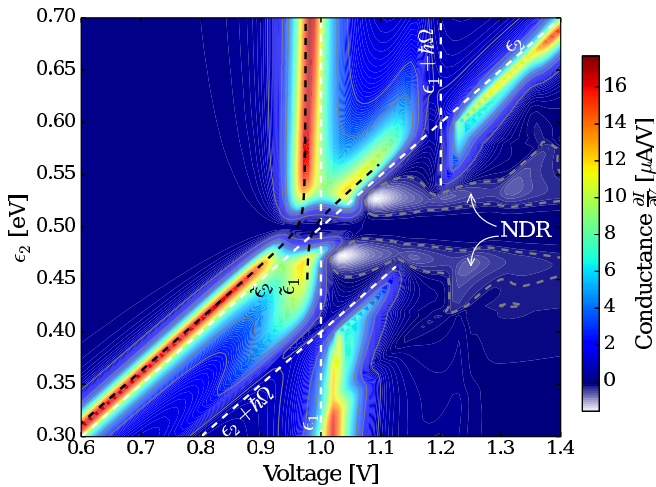

FIG. 9. (Color online) Conductance map of the system DESNONAD for varying electronic energy ϵ_2. The purely nonadiabatic electronic-vibrational coupling strength is $M_{12} = 0.05$ eV. The white dashed lines indicate the position of the electronic resonances. The positions of the corresponding two-level system with empirically determined constant coupling strength $\Delta = 0.0075$ eV are marked by black dashed lines in the relevant region. The light colors on the right-hand side of the plot close to the line $\epsilon_2 = \epsilon_1 = 0.5$ eV indicate regions of negative differential resistance.

approximation, the location of the electronic resonances in the conductance map of the interacting system can be described by the noninteracting model with an effective coupling of $\Delta = 0.0075$ eV (black dashed lines in Fig. 9).

In addition to the level splitting, the interaction between the molecular electronic states leads to new eigenstates. According to Eq. (35), one of the new eigenstates couples more strongly to the left lead but more weakly to the right lead, whereas the other eigenstate couples more strongly to the right lead but more weakly to the left lead, which results in an overall suppression of the current. In the limit $\epsilon_1 = \epsilon_2$, the two new eigenstates couple either to the left or the right lead such that the current vanishes. This behavior is also found in the noninteracting system without interstate coupling ($\Delta = 0$) for $\epsilon_1 = \epsilon_2$. In this case, however, the current disappears due to perfect destructive interference between the two transport channels through the individual electronic states. Assuming that the nonadiabatic electronic-vibrational coupling provided a source of decoherence, as was found for adiabatic electronic-vibrational coupling [33], the perfect destructive interference would be diminished, leading to a finite current for $\epsilon_1 = \epsilon_2$. This is, however, not observed in the data presented in Fig. 9. This is due to the fact that, in contrast to adiabatic electronic-vibrational coupling, nonadiabatic coupling does not provide information on the specific path (electronic state) an electron has taken through the molecular bridge and thus does not act as a direct source of decoherence. Rather, it mixes the two electronic states. This is discussed in more detail in Sec. III B 3.

The NDR phenomenon observed in Fig. 9 cannot be explained by the simple toy model of Sec. III B 1 with constant coupling Δ between the two electronic states. The nonadiabatic interaction between the electronic and vibrational degrees of freedom results in an effective interstate coupling, which depends on the population of the electronic states and thus on the bias voltage. Specifically, in the model system DESNONAD an increase in the population of the electronic states, obtained for bias voltages beyond the onset of resonant transport, leads effectively to a stronger interstate coupling. The resulting enhanced mixing of the electronic levels causes a decreased current, i.e., NDR. As this mechanism is less effective for larger energy differences $|\epsilon_2 - \epsilon_1|$, NDR can be observed only for parameter regimes close to $\epsilon_1 = \epsilon_2$.

3. Influence of adiabatic and nonadiabatic electronic-vibrational interactions

Finally, we study the influence of nonadiabatic electronic-vibrational coupling on a quasidegenerate electronic system in the presence of adiabatic vibrational interaction. To this end, we extend the model system DESVIB introduced by Härtle *et al.* [33] by a nonadiabatic electronic-vibrational coupling of varying strength (see Table I).

The results obtained for the current-voltage characteristics of this model, depicted in Fig. 10, show that the system with electronic-vibrational interaction allows for a significantly higher current than the purely electronic model. Thereby, the system with only adiabatic coupling to the vibrations ($M_{12} = 0$) is the best conductor, whereas the current decreases with increasing nonadiabatic electronic-vibrational coupling strength M_{12}. The overall shape of the current-voltage
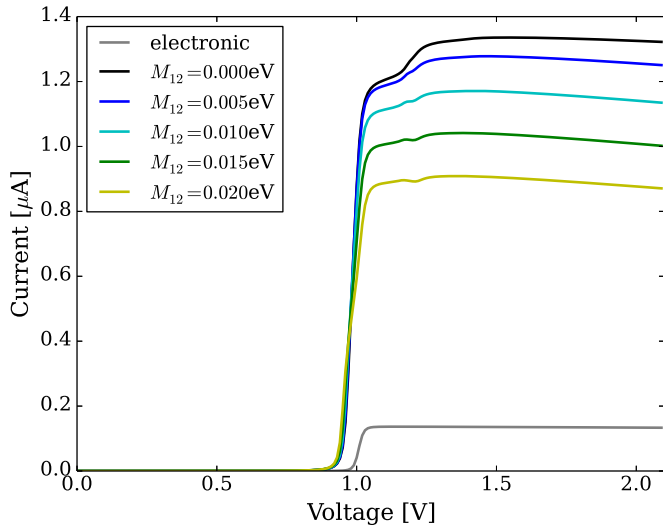
FIG. 10. (Color online) Current-voltage characteristics of the system DESVIB for varying nonadiabatic electronic-vibrational coupling. The gray line gives the current without electronic-vibrational interaction, the black line is the current for the system with purely adiabatic electronic-vibrational coupling, and the blue and green lines corresponds to the current of the system with different nonadiabatic electronic-vibrational coupling ranging from $M_{12} = 0.005$ eV to $M_{12} = 0.02$ eV.
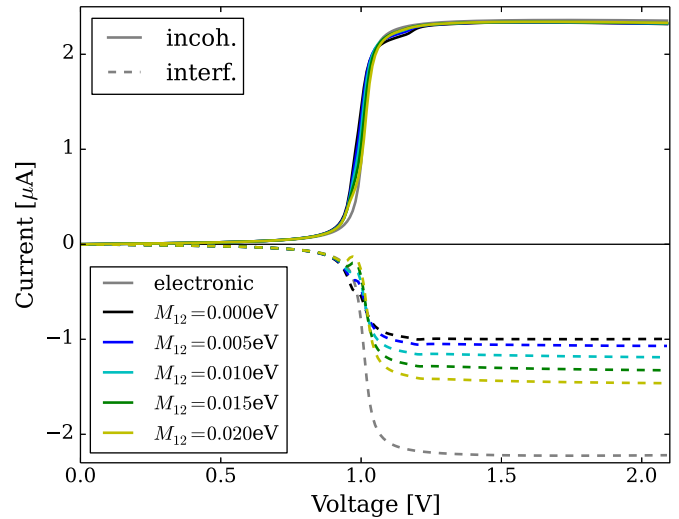

FIG. 11. (Color online) Interference (dashed lines) and incoherent (solid lines) contributions to the currents of the system DESVIB for varying nonadiabatic electronic-vibrational coupling strength M_{12}.

characteristics is rather insensitive to the strength of nonadiabatic coupling. The minor changes in the overall shape of the current can be traced back to the interplay between adiabatic and nonadiabatic electronic-vibrational interactions, as already discussed in preceding sections.

As was studied in detail in Refs. [30,33], the interaction between electrons and nuclei increases the current in the system with purely adiabatic coupling ($M_{12} = 0$) because the vibrations provide which-path information, thus quenching the destructive interference present in the noninteracting system [33]. To analyze the influence of nonadiabatic electronic-vibrational coupling, we separate the current into incoherent and interference contributions according to Eqs. (23) and (24). The results in Fig. 11 show that nonadiabatic coupling reduces the interference contribution to the current, while the incoherent contribution is essentially unaffected. This can be rationalized in the following way. State-specific adiabatic electronic-vibrational coupling provides information on the specific path (electronic state) an electron has taken through the molecular bridge and thus acts as a direct source of decoherence. Nonadiabatic electronic-vibrational coupling, on the other hand, mixes the two electronic states and thus tends to quench which-path information. As a result, in a system with strong decoherence such as the model DESVIB, the current decreases with increasing nonadiabatic coupling.

IV. CONCLUSIONS

We have investigated the influence of nonadiabatic electronic-vibrational interactions on the transport properties of single-molecule junctions. Employing nonequilibrium Green's functions within the self-consistent Born approximation to simulate the current-voltage characteristics, we studied model molecular junctions comprising two electronic states coupled to a vibrational mode. Thereby, two different types of molecular junctions were considered, which differ by the energy spacing of the electronic states.

For molecular junctions with well-separated electronic states, an analytical analysis of the most important vibrational effects shows that nonadiabatic coupling may have pronounced effects if the resonance condition $\epsilon_i + \hbar\Omega \approx \epsilon_j$ with $i \neq j$ is fulfilled. Numerical calculations revealed the fundamental differences between adiabatic and nonadiabatic electronic-vibrational couplings, which manifest themselves in a different dependence of the transport properties on the vibrational energy $\hbar\Omega$ and in transport channels caused by the level-mixing in the case of nonadiabatic coupling. The latter mechanism can lead to an asymmetric current-voltage characteristic, i.e., rectifying behavior, in junctions with state-specific asymmetric coupling to the leads. Moreover, the interplay between adiabatic and nonadiabatic vibrational effects results in interference effects that change the current depending on the relative sign between the different vibrational couplings.

To analyze the effect of nonadiabatic electronic-vibrational interactions in molecular junctions with quasidegenerate electronic levels, we considered model systems which were previously shown to exhibit significant interference and decoherence effects [33]. Our study shows that purely nonadiabatic vibrational coupling in these systems results in an avoided crossing of the energy levels and tends to suppress the current. Moreover, the specific nature of the nonadiabatic electronic-vibrational interaction can result in NDR as a consequence of charging the molecule. In contrast to state-specific adiabatic coupling, nonadiabatic coupling does not provide a decoher-

ence mechanism. Rather, it causes mixing of the electronic states and thus quenches which-path information.

In the present work we have considered molecular junctions with a single vibrational mode. In polyatomic molecules, multiple vibrational modes may interact with the electronic degrees of freedom. In this case intersections of potential-energy surfaces are possible and may result in strong nonadiabatic coupling. The resulting phenomena are well studied in molecules in the gas phase and in solution [52]. The investigation of these effects under nonequilibrium conditions in molecular junction is an interesting topic for future research.

APPENDIX: IDENTIFICATION OF IMPORTANT TRANSPORT PROCESSES FOR SYSTEMS WITH WELL-SEPARATED ELECTRONIC STATES

In Sec. III A 1, we identified the most important effects of electronic-vibrational interactions by expanding the current in the couplings M_{ij} and V_{ij}. Considering well-separated electronic systems and using the strongly peaked nature of Green's functions, we employed an additional approximation beyond perturbation theory in Sec. III A 1. Specifically, a simplification for the expression for the current was obtained by neglecting the product of two Green's functions of different electronic states for a fixed energy. Depending on the system under consideration, the coupling to the leads can result in relatively large off-diagonal Green's function elements such that completely disregarding the product of two Green's functions of different electronic states at the same energy may not be valid. Nevertheless, the coupling to the leads still represents a perturbation to the system such that an improved expression for the current can be derived by additionally allowing for contributions that contain the product with one Green's function of another electronic state at a given energy. A generalization of this approach is straightforward. The elastic correction to the current and the inelastic current read

$$
\delta I_{\text{L el}} \approx \frac{e}{2\pi\hbar} \sum_{i,j\neq i} \int \Sigma^<_{\text{L}\,ij}(\epsilon) \Bigg(G^{0r}_{jj}(\epsilon)^2 \bigg[|M_{ji}|^2 \mathcal{G}^{0r}_{ii}(\epsilon) + M^2_{jj}\mathcal{G}^{0r}_{jj}(\epsilon) + \sum_{k\neq i\wedge j} |M_{jk}|^2 \mathcal{G}^{0r}_{kk}(\epsilon) \bigg] G^{0a}_{ii}(\epsilon) + \text{H.c.} \Bigg) \Sigma^>_{\text{R}\,ji}(\epsilon)
$$

$$
+ \Sigma^<_{\text{L}\,ii}(\epsilon) \Bigg(\big|G^{0r}_{ii}(\epsilon)\big|^2 \bigg[M_{ii}M_{ij}\mathcal{G}^{0r}_{ii}(\epsilon) + M_{ij}M_{jj}\mathcal{G}^{0r}_{jj}(\epsilon) + \sum_{k\neq i\wedge j} M_{ik}M_{kj}\mathcal{G}^{0r}_{kk}(\epsilon) \bigg] G^{0r}_{jj}(\epsilon) + \text{H.c.} \Bigg) \Sigma^>_{\text{R}\,ji}(\epsilon)
$$

$$
+ \Sigma^<_{\text{L}\,ij}(\epsilon) \Bigg(G^{0r}_{jj}(\epsilon) \bigg[M_{ji}M_{ii}\mathcal{G}^{0r}_{ii}(\epsilon) + M_{jj}M_{ji}\mathcal{G}^{0r}_{jj}(\epsilon) + \sum_{k\neq i\wedge j} M_{jk}M_{ki}\mathcal{G}^{0r}_{kk}(\epsilon) \bigg] \big|G^{0r}_{ii}(\epsilon)\big|^2 + \text{H.c.} \Bigg) \Sigma^>_{\text{R}\,ii}(\epsilon)\, d\epsilon
$$

$$
+ \delta I^{\text{sep}}_{\text{L el}} + R + O(M^4 V^6), \tag{A1}
$$

$$
I_{\text{L inel}} \approx I^{\text{sep}}_{\text{L inel}} + \frac{e}{2\pi\hbar} \int \sum_{i,k\neq i} \Sigma^<_{\text{L}\,ii}(\epsilon) \big|G^{0r}_{ii}(\epsilon)\big|^2 \bigg[M_{ii}M_{ki}\mathcal{G}^{0>}_{ik}(\epsilon) + M_{ik}M_{ii}\mathcal{G}^{0>}_{ki}(\epsilon) + \sum_{l\neq k\wedge i} M_{ik}M_{li}\mathcal{G}^{0>}_{kl}(\epsilon) \bigg]
$$

$$
+ \sum_{i,j\neq i} \Sigma^<_{\text{L}\,ij}(\epsilon) G^{0r}_{jj}(\epsilon) \bigg[M_{ji}M_{ii}\mathcal{G}^{0>}_{ii}(\epsilon) + M_{jj}M_{ji}\mathcal{G}^{0>}_{jj}(\epsilon) + \sum_{k\neq i\wedge j} M_{jk}M_{ki}\mathcal{G}^{0>}_{kk}(\epsilon) \bigg] G^{0a}_{ii}(\epsilon)\, d\epsilon + O(M^4 V^6). \tag{A2}
$$

Here, $\delta I^{\text{sep}}_{\text{L el}}$ and $I^{\text{sep}}_{\text{L inel}}$ are the contributions to the current as specified in Eqs. (29) and (30), and R denotes the influence of the Hartree term which leads to further renormalization of the electronic levels and which will be neglected here for the sake of readability. In this approximation, the expressions for the currents incorporate a variety of different terms. The equations can be separated into three different parts corresponding to different type of effects of the vibrations on the current.

The first effect is an enhancement of purely adiabatic or nonadiabatic vibrational effects identified in Sec. III A 1. These terms are proportional to M^2_{ii} and $|M_{ij}|^2$ with $i \neq j$,

respectively. The second type mixes the adiabatic and the nonadiabatic electronic-vibrational coupling. The corresponding terms are proportional to $M_{ii}M_{ij}$ with $i \neq j$. Notice that these summands are also proportional to off-diagonal elements of the self-energy for the coupling to the leads. As discussed in Sec. III A 4, this combined action of adiabatic and nonadiabatic electronic-vibrational interactions can have a strong influence on the current. The last kind of process that influences the current in this approximation depends on three different electronic states. The corresponding terms are proportional to $M_{ik}M_{kj}$ with $i \neq j \neq k$ and rely only on nonadiabatic electronic-vibrational interactions. They describe transport

processes, where an electron is scattered from an initial to a final electronic state via another different state. They represent therefore a more general form of the purely nonadiabatic electronic-vibrational processes identified in Sec. III A 1.

While the latter type of process does not contribute in our models with two electronic levels, it may be of importance in molecular junctions with multiple closely lying electronic states.

---

[1] M. A. Reed, C. Zhou, C. J. Muller, T. P. Burgin, and J. M. Tour, Science **278**, 252 (1997).

[2] J. Reichert, R. Ochs, D. Beckmann, H. B. Weber, M. Mayor, and H. v. Löhneysen, Phys. Rev. Lett. **88**, 176804 (2002).

[3] T. Böhler, J. Grebing, A. Mayer-Gindner, H. von Löhneysen, and E. Scheer, Nanotechnology **15**, 465 (2004).

[4] L. Venkataraman, J. E. Klare, C. Nuckolls, M. S. Hybertsen, and M. L. Steigerwald, Nature (London) **442**, 904 (2006).

[5] D. R. Ward, N. J. Halas, J. W. Ciszek, J. M. Tour, Y. Wu, P. Nordlander, and D. Natelson, Nano Lett. **8**, 919 (2008).

[6] F. Mohn, J. Repp, L. Gross, G. Meyer, M. S. Dyer, and M. Persson, Phys. Rev. Lett. **105**, 266102 (2010).

[7] D. Secker, S. Wagner, S. Ballmann, R. Härtle, M. Thoss, and H. B. Weber, Phys. Rev. Lett. **106**, 136807 (2011).

[8] Y. Kim, H. Song, F. Strigl, H.-F. Pernau, T. Lee, and E. Scheer, Phys. Rev. Lett. **106**, 196804 (2011).

[9] S. Ballmann, W. Hieringer, R. Härtle, P. B. Coto, M. R. Bryce, A. Grling, M. Thoss, and H. B. Weber, Phys. Status Solidi B **250**, 2452 (2013).

[10] A. Aviram and M. A. Ratner, Chem. Phys. Lett. **29**, 277 (1974).

[11] A. Nitzan, Annu. Rev. Phys. Chem. **52**, 681 (2001).

[12] C. Joachim and M. A. Ratner, Proc. Natl. Acad. Sci. USA **102**, 8801 (2005).

[13] G. Cuniberti, G. Fagas, and K. Richter, *Introducing Molecular Electronics* (Springer, Heidelberg, 2006).

[14] J. C. Cuevas and E. Scheer, *Molecular Electronics: An Introduction to Theory and Experiment* (World Scientific, Singapore, 2010).

[15] S. Braig and K. Flensberg, Phys. Rev. B **68**, 205324 (2003).

[16] S. W. Wu, G. V. Nazin, X. Chen, X. H. Qiu, and W. Ho, Phys. Rev. Lett. **93**, 236802 (2004).

[17] M. Elbing, R. Ochs, M. Koentopp, M. F. C. von Hänisch, F. Weigend, F. Evers, H. Weber, and M. Mayor, Proc. Natl. Acad. Sci. USA **102**, 8815 (2005).

[18] I. Diez-Perez, J. Hihath, Y. Lee, L. Yu, L. Adamska, M. A. Kozhushner, I. I. Oleynik, and N. Tao, Nat. Chem. **1**, 635 (2009).

[19] R. Härtle and M. Thoss, Phys. Rev. B **83**, 115414 (2011).

[20] A. S. Blum, J. G. Kushmerick, D. P. Long, C. H. Patterson, J. C. Jang, J. C. Henderson, Y. Yao, J. M. Tour, R. Shashidhar, and B. R. Ratna, Nat. Mater. **4**, 167 (2005).

[21] B.-Y. Choi, S.-J. Kahng, S. Kim, H. Kim, H. W. Kim, Y. J. Song, J. Ihm, and Y. Kuk, Phys. Rev. Lett. **96**, 156106 (2006).

[22] S. Y. Quek, M. Kamenetska, M. L. Steigerwald, H. J. Choi, S. G. Louie, M. S. Hybertsen, J. B. Neaton, and L. Venkataraman, Nat. Nanotechnol. **4**, 230 (2009).

[23] V. Meded, A. Bagrets, A. Arnold, and F. Evers, Small **5**, 2218 (2009).

[24] C. Benesch, M. F. Rode, M. Čížek, R. Härtle, O. Rubio-Pons, M. Thoss, and A. L. Sobolewski, J. Phys. Chem. C **113**, 10315 (2009).

[25] S. J. van der Molen and P. Liljeroth, J. Phys. Condens. Matter **22**, 133001 (2010).

[26] O. Hod, R. Baer, and E. Rabani, Phys. Rev. Lett. **97**, 266803 (2006).

[27] G. C. Solomon, D. Q. Andrews, R. P. Van Duyne, and M. A. Ratner, J. Am. Chem. Soc. **130**, 7788 (2008).

[28] G. Begemann, D. Darau, A. Donarini, and M. Grifoni, Phys. Rev. B **77**, 201406 (2008).

[29] T. Markussen, R. Stadler, and K. S. Thygesen, Nano Lett. **10**, 4260 (2010).

[30] R. Härtle, M. Butzin, O. Rubio-Pons, and M. Thoss, Phys. Rev. Lett. **107**, 046802 (2011).

[31] S. Ballmann, R. Härtle, P. B. Coto, M. Elbing, M. Mayor, M. R. Bryce, M. Thoss, and H. B. Weber, Phys. Rev. Lett. **109**, 056801 (2012).

[32] C. M. Guedon, H. Valkenier, T. Markussen, K. S. Thygesen, J. C. Hummelen, and S. J. van der Molen, Nat. Nanotechnol. **7**, 305 (2012).

[33] R. Härtle, M. Butzin, and M. Thoss, Phys. Rev. B **87**, 085422 (2013).

[34] J. Gaudioso, L. J. Lauhon, and W. Ho, Phys. Rev. Lett. **85**, 1918 (2000).

[35] B. W. Heinrich, M. V. Rastei, D.-J. Choi, T. Frederiksen, and L. Limot, Phys. Rev. Lett. **107**, 246801 (2011).

[36] M. H. Hettler, W. Wenzel, M. R. Wegewijs, and H. Schoeller, Phys. Rev. Lett. **90**, 076805 (2003).

[37] J. Koch and F. von Oppen, Phys. Rev. B **72**, 113308 (2005).

[38] E. Pop, D. Mann, J. Cao, Q. Wang, K. Goodson, and H. Dai, Phys. Rev. Lett. **95**, 155505 (2005).

[39] S. Sapmaz, P. Jarillo-Herrero, Y. M. Blanter, C. Dekker, and H. S. J. van der Zant, Phys. Rev. Lett. **96**, 026801 (2006).

[40] A. Zazunov, D. Feinberg, and T. Martin, Phys. Rev. B **73**, 115405 (2006).

[41] B. Muralidharan and S. Datta, Phys. Rev. B **76**, 035432 (2007).

[42] O. Tal, M. Krieger, B. Leerink, and J. M. van Ruitenbeek, Phys. Rev. Lett. **100**, 196804 (2008).

[43] M. Leijnse and M. R. Wegewijs, Phys. Rev. B **78**, 235424 (2008).

[44] M. Galperin, M. A. Ratner, and A. Nitzan, J. Phys. Condens. Matter **19**, 103201 (2007).

[45] L. J. Lauhon and W. Ho, Phys. Rev. Lett. **84**, 1527 (2000).

[46] A. Mitra, I. Aleiner, and A. J. Millis, Phys. Rev. B **69**, 245302 (2004).

[47] J. Koch and F. von Oppen, Phys. Rev. Lett. **94**, 206804 (2005).

[48] M. Galperin, A. Nitzan, and M. A. Ratner, Phys. Rev. B **73**, 045314 (2006).

[49] R. Härtle, R. Volkovich, M. Thoss, and U. Peskin, J. Chem. Phys. **133**, 081102 (2010).

[50] E. Y. Wilner, H. Wang, M. Thoss, and E. Rabani, Phys. Rev. B **89**, 205129 (2014).

[51] H. Köuppel, W. Domcke, and L. S. Cederbaum, Adv. Chem. Phys. **57**, 59 (1984).

[52] W. Domcke, D. R. Yarkony, and H. Köppel, *Conical Intersections: Electronic Structure, Dynamics and Spectroscopy* (World Scientific, Singapore, 2004).

[53] F. Reckermann, M. Leijnse, M. R. Wegewijs, and H. Schoeller, Europhys. Lett. **83**, 58001 (2008).

[54] T. Frederiksen, K. J. Franke, A. Arnau, G. Schulze, J. I. Pascual, and N. Lorente, Phys. Rev. B **78**, 233401 (2008).

[55] M. G. Schultz, T. S. Nunner, and F. von Oppen, Phys. Rev. B **77**, 075323 (2008).

[56] J. E. Han, Phys. Rev. B **81**, 113106 (2010).

[57] J. Repp, P. Liljeroth, and G. Meyer, Nat. Phys. **6**, 975 (2010).

[58] M. Paulsson, T. Frederiksen, and M. Brandbyge, Nano Lett. **6**, 258 (2005).

[59] J. Hihath, C. Bruot, and N. Tao, ACS Nano **4**, 3823 (2010).

[60] R. Avriller and T. Frederiksen, Phys. Rev. B **86**, 155411 (2012).

[61] M. Bürkle, J. K. Viljas, T. J. Hellmuth, E. Scheer, F. Weigend, G. Schön, and F. Pauly, Phys. Status Solidi B **250**, 2468 (2013).

[62] V. May, Phys. Rev. B **66**, 245411 (2002).

[63] J. N. Pedersen and A. Wacker, Phys. Rev. B **72**, 195330 (2005).

[64] U. Harbola, M. Esposito, and S. Mukamel, Phys. Rev. B **74**, 235309 (2006).

[65] M. Čížek, M. Thoss, and W. Domcke, Phys. Rev. B **70**, 125406 (2004).

[66] M. Caspary Toroker and U. Peskin, J. Chem. Phys. **127**, 154706 (2007).

[67] N. A. Zimbovskaya and M. M. Kuklja, J. Chem. Phys. **131**, 114703 (2009).

[68] R. Jorn and T. Seideman, J. Chem. Phys. **131**, 244114 (2009).

[69] L. Mühlbacher and E. Rabani, Phys. Rev. Lett. **100**, 176403 (2008).

[70] S. Weiss, J. Eckel, M. Thorwart, and R. Egger, Phys. Rev. B **77**, 195316 (2008).

[71] H. Wang and M. Thoss, J. Chem. Phys. **131**, 024114 (2009).

[72] C. Verdozzi, G. Stefanucci, and C.-O. Almbladh, Phys. Rev. Lett. **97**, 046603 (2006).

[73] B. Li, E. Y. Wilner, M. Thoss, E. Rabani, and W. H. Miller, J. Chem. Phys. **140**, 104110 (2014).

[74] A. B. Migdal, Sov. Phys. JETP **7**, 996 (1958).

[75] C. Caroli, R. Combescot, P. Nozieres, and D. Saint-James, J. Phys. C **5**, 21 (1972).

[76] P. Hyldgaard, S. Hershfield, J. Davies, and J. Wilkins, Ann. Phys. (NY) **236**, 1 (1994).

[77] A. Pecchia and A. D. Carlo, Rep. Prog. Phys. **67**, 1497 (2004).

[78] D. A. Ryndyk, M. Hartung, and G. Cuniberti, Phys. Rev. B **73**, 045420 (2006).

[79] A. Ueda and M. Eto, New J. Phys. **9**, 119 (2007).

[80] R. Härtle, C. Benesch, and M. Thoss, Phys. Rev. B **77**, 205314 (2008).

[81] O. Entin-Wohlman, Y. Imry, and A. Aharony, Phys. Rev. B **80**, 035417 (2009).

[82] F. Haupt, T. Novotný, and W. Belzig, Phys. Rev. Lett. **103**, 136601 (2009).

[83] L. S. Cederbaum and W. Domcke, J. Chem. Phys. **60**, 2878 (1974).

[84] I. G. Lang and Y. A. Firsov, Sov. Phys. JETP **16**, 1301 (1963).

[85] G. D. Mahan, *Many-Particle Physics* (Plenum, New York, 1993).

[86] J. Koch, M. Semmelhack, F. von Oppen, and A. Nitzan, Phys. Rev. B **73**, 155306 (2006).

[87] R. Härtle, C. Benesch, and M. Thoss, Phys. Rev. Lett. **102**, 146801 (2009).

[88] G. Romano, A. Gagliardi, A. Pecchia, and A. Di Carlo, Phys. Rev. B **81**, 115438 (2010).

[89] R. Härtle and M. Thoss, Phys. Rev. B **83**, 125419 (2011).

[90] R. Volkovich, R. Härtle, M. Thoss, and U. Peskin, Phys. Chem. Chem. Phys. **13**, 14333 (2011).

[91] A. J. White and M. Galperin, Phys. Chem. Chem. Phys. **14**, 13809 (2012).

[92] A. J. White, M. A. Ochoa, and M. Galperin, J. Phys. Chem. C **118**, 11159 (2014).

[93] L. P. Kadanoff and G. Baym, *Quantum Statistical Mechanics: Green's Function Methods in Equilibrium and Non-equilibrium Problems* (Benjamin, New York, 1962).

[94] L. V. Keldysh, Zh. Eksp. Teor. Fiz. **47**, 1515 (1964).

[95] D. C. Langreth, in *Linear and Nonlinear Electron Transport in Solids*, NATO Advanced Studies Institute, Series B: Physics Vol. 17 (Plenum, New York, 1976), pp. 3–32.

[96] T. Frederiksen, Master's thesis, Technical University of Denmark, 2004.

[97] H. J. W. Haug and A.-P. Jauho, *Quantum Kinetics in Transport and Optics of Semiconductors*, Springer Series in Solid-State Sciences (Springer, Berlin, 2008).

[98] U. Peskin, J. Phys. B **43**, 153001 (2010).

[99] M. Galperin, M. A. Ratner, and A. Nitzan, J. Chem. Phys. **121**, 11965 (2004).

[100] J. R. Schrieffer, *Theory of Superconductivity* (Benjamin, New York, 1964).

[101] W. Lee, N. Jean, and S. Sanvito, Phys. Rev. B **79**, 085120 (2009).

[102] L. K. Dash, H. Ness, and R. W. Godby, J. Chem. Phys. **132**, 104113 (2010).

[103] L. K. Dash, H. Ness, and R. W. Godby, Phys. Rev. B **84**, 085433 (2011).

[104] Y. Meir and N. S. Wingreen, Phys. Rev. Lett. **68**, 2512 (1992).

[105] H. Mera, M. Lannoo, C. Li, N. Cavassilas, and M. Bescond, Phys. Rev. B **86**, 161404 (2012).

[106] L. C. Davis, Phys. Rev. B **2**, 1714 (1970).

[107] H. Vazquez, R. Skouta, S. Schneebeli, M. Kamenetska, R. Breslow, L. Venkataraman, and M. S. Hybertsen, Nat. Nanotechnol. **7**, 663 (2012).

[108] G. C. Solomon, A. Gagliardi, A. Pecchia, T. Frauenheim, A. Di Carlo, J. R. Reimers, and N. S. Hush, Nano Lett. **6**, 2431 (2006).

[109] G. C. Solomon, D. Q. Andrews, T. Hansen, R. H. Goldsmith, M. R. Wasielewski, R. P. Van Duyne, and M. A. Ratner, J. Chem. Phys. **129**, 054701 (2008).

[110] M. Galperin, A. Nitzan, M. A. Ratner, and D. R. Stewart, J. Phys. Chem. B **109**, 8519 (2005).